The Behaviour of Population in a Plasma Interacting with an Atomic Gas

Utaro Furukane
Department of Physics, College of General Education, Ehime University, Matsuyama 790, Japan

Toshiatsu Oda
Faculty of Science, Hiroshima University, Hiroshima 730, Japan

Z. Naturforsch. **39 a**, 132–141 (1984); received October 11, 1983

The processes leading to the population inversion are investigated in a recombining hydrogen plasma which is interacting with a cool and dense neutral hydrogen gas by using the rate equations on the basis of a collisional-radiative (CR) model and the energy equations for electrons, ions and neutral particles. The quasi-steady state (QSS) approximation is used only for the levels i lying above a certain level i^* which is not the first excited level. The calculations have shown that the quasi-steady state cannot be realized while intense energy-flows due to the collisional processes exist between different kinds of the particles such as the electrons and the ions in the plasma, and that the population inversion is realized only in the quasi-steady state following the transient phase. The effects of the initial conditions of the hydrogen plasma and of the introduced neutral hydrogen gas on the overpopulation density are also discussed.

1. Introduction

Recombining plasmas in which the population inversion is generated have been already recognized by Gudzenko and Shelepin [1] to be promising as a laser-acting medium.

The quasi-steady state (QSS) assumption for all excited levels has been widely used in most theoretical investigations on population inversion and laser oscillation [2–6]. The mechanism generating the population inversion between the lower lying levels in QSS is explained as follows: The upper one of the two levels of interest is populated mainly due to cascade collisional decay from the higher excited levels where the electrons are captured by the three-body recombination, and the lower one is significantly depopulated by the radiative deexcitation.

The region of the plasma parameters for generating the population inversion of the recombining plasma in QSS has been investigated by Bohn [7] and Furukane et al. [8–10]. For these recombining plasmas, the plasma conditions to obtain the high gains necessary for the laser oscillation have been also discussed by Bohn [7] and by Oda and Furukane [11].

Experimental investigations have been reported for generating population inversions between excited states of the hydrogen atom and hydrogen-like ions in recombining plasmas and laser oscillations based on the population inversions: Hoffman and Bohn [12] observed population inversion between levels with principal quantum numbers $j = 3$ and 5 of the hydrogen atom during the plasma recombination phase in an expansion-flow-system. The laser oscillations were reported to occur in the expanding plasmas for an ArIII line (Campbell et al. [2]), and also for the P_γ line of the hydrogen atom (Hara et al. [3]). n the other hand, Sato et al. [5] investigated a stationary population inversion between low lying levels of He^+ in the TPD-I magnetically confined recombining plasma column which was interacting with neutral helium gas without any expansion. TPD-I is a quiescent high-density plasma source. It consists basically of two parts, namely, the discharge region with the cathode at the center of the cusped magnetic field and the plasma column region with the axial magnetic field. The details have already been published [13]. Since the charged particle density in the column does not decrease along the axis as in the expanding plasma, there is the possibility of obtaining a higher gain and a VUV laser oscillation. Moreover, the TPD-I plasma is superior to the expanding plasma in that the plasma parameters are easily controlled and reproducible, and even one-dimensional consideration on the basis of the CR model can yield good theoretical predictions. The cooling rate of the TPD-I recombining plasma which is interacting with cool and

Reprint requests to Dr. U. Furukane, College of General Education, Ehime University, Matsuyama 790, Japan.

0340-4811 / 84 / 0200-0132 $ 01.3 0/0. – Please order a reprint rather than making your own copy.

dense neutral gas is expected to be much greater, since the relevant collisional cross sections are very large. This makes QSS approximation unsuitable for investigating the cooling processes.

In the present paper, our purpose is to investigate the cooling process of the TPD-I plasma, as previously stated, by using the rate equations on the basis of a CR model without the quasi-steady state approximation and thereby to elucidate the processes leading to the population inversion. The energy equations for the electrons, ions and atoms in the plasma are also jointly used. We make a simplified model of a recombining plasma in TPD-I as follows: low temperature and high density gas of hydrogen atoms is mixed with a cylindrical hydrogen plasma of high electron temperature. Radial distributions of the charged particles and the neutral atoms are all assumed to be of bell-shaped form with a mean radius of 0.84 cm [14].

We present numerical results calculated on the center axis of the plasma, and demonstrate the processes yielding the population inversion in the hydrogen plasma. We also discuss the effects of the initial conditions of the plasma and the introduced neutral gas on the overpopulation density [11] obtained.

2. Basic equation

The *elastic* collisional processes are considered for collisions between electrons and atoms, electrons and ions, and atoms and ions. The *inelastic* collisional and radiative processes considered here are as follows:

(a) $H_i + e \rightleftarrows H_k + e \quad (k > i)$,

(b) $H_i + e \rightleftarrows H_+ + e + e$,

(c) $H_+ + e \rightarrow H_i + h\nu$,

(d) $H_i + N \rightleftarrows H_k + N \quad (k > i)$,

(e) $H_i + N \rightleftarrows H_+ + e + N$,

(f) $H_k \rightarrow H_i + h\nu \quad (k > i)$,

(g) $H_1 + h\nu \rightarrow H_i \quad (i > 2)$,

where H_i denotes an excited hydrogen atom in level i, H_+ an ionized hydrogen atom, e an electron, N a hydrogen atom in the ground state, and $h\nu$ a photon. Let the plasma flow along the z axis be constant with a speed of v_0. We consider a coordinate fixed to the flow, i.e., $\frac{d}{dt} = \frac{\partial}{\partial t} + v_0 \frac{\partial}{\partial z}$.

The rate equation for the population density n_i of H_i $(1 \leqq i \leqq 20)$ is given by [10]:

$$\frac{dn_i}{dt} = \sum_{j=1}^{20} (a_{ij} + n_1 a'_{ij}) n_j + (\delta_i + n_1 \delta'_i), \quad 1 \leqq i \leqq 20. \tag{1}$$

Here, the maximum quantum number is chosen to be 20 as by Cacciatore and Capitelli [15]. The coefficients a_{ij} and δ_i are given in terms of the radiative transition probability A_{ij} $(i < j)$ and the optical escape factors Λ_{ij}, Λ_i and the rate coefficients for electron collisional ionization K_{ic} and recombination K_{ci}, electron collisional excitation C_{ij} $(i < j)$ and deexcitation F_{ji} $(i < j)$ and radiative recombination β_i as follows:

$$a_{ij} = n_e C_{ji} \quad \text{for} \quad i > j,$$

$$a_{ii} = -n_e (K_{ic} + \sum_{j>i} C_{ij} + \sum_{j<i} F_{ij}) - \sum_{j<i} \Lambda_{ji} A_{ji},$$

$$a_{ij} = \Lambda_{ij} A_{ij} + n_e F_{ji} \quad \text{for} \quad i < j,$$

$$\delta_i = n_e^2 (n_e K_{ci} + \Lambda_i \beta_i).$$

The coefficients a'_{ij} and δ'_i are given by the rate coefficients for atomic collisional ionization K^0_{ic} and recombination K^0_{ci}, atomic collisional excitation C^0_{ij} $(i < j)$ and deexcitation F^0_{ji} $(i < j)$ as follows:

$$a'_{ij} = C^0_{ji} \quad \text{for} \quad i > j,$$

$$a_{ii} = -(K^0_{ic} + \sum_{j>i} C^0_{ij} + \sum_{j<i} F^0_{ij}),$$

$$a'_{ij} = F^0_{ij} \quad \text{for} \quad i < j,$$

$$\delta_i = n_e^2 K^0_{ci}.$$

In Eq. (1) the term for the excited particle flux in radial direction can be neglected because of the small relaxation length of the excited states [5, 16]. In the neighbourhood of the center axis of the plasma, the radial distribution of the electron density and temperature have been observed to be almost flat in the neighbourhood of the center axis as is shown in Fig. 7 of [13]. Thus, the ground state particle flux in radial direction can be neglected in the neighbourhood of the center axis of the plasma column.

The electron density n_e is given by

$$\frac{dn_e}{dt} = -\sum_{j=1}^{20} \frac{dn_j}{dt}. \tag{2}$$

We use the following energy equation:

$$\frac{d}{dt} (\tfrac{3}{2} n_\chi T_\chi) = R_\chi + Q_\chi, \tag{3}$$

where the terms of spatial divergence are neglected as in (1), and $3n_\chi T_\chi/2$ denotes the thermal energy, the suffix χ represents a species of the particles; e, i and a indicate electron, ion and atom, respectively. However, to avoid confusion, we use the notation n^+ for the ion density. Here, R_χ denotes the rate of increase of the thermal energy due to the elastic collisions and Q_χ denotes that due to the inelastic collisions. Detailed descriptions of (3) are given in Appendix A.

The optical escape factors Λ_{1j} ($j \geqq 2$) for the lines (assuming Doppler profiles for the Lyman series) are calculated simultaneously with (1), (2), and (3) in the manner described in a previous paper [10]. All the other optical escape factors Λ_{ij} ($i \geqq 2$, for all j) are put equal to unity; that is, the plasma is considered to be optically thin except for the Lyman series.

As initial conditions of our numerical calculations, we assume that the hydrogen plasma in a stationary state whose electron and ion temperatures and electron density are T_{e0}, T_{i0} and n_{e0} is brought into interaction with a neutral hydrogen gas of high density ($n_1 = n_{10}$) at $t = 0$, all the hydrogen atoms being in the ground state at an initial atom-temperature of T_{a0}. We have made the calculations for three initial temperature and density conditions shown in Table 1. They are chosen in order to see the difference in the cooling speed between the main processes leading to the population inversion. In case I, the initial neutral gas density n_{10} is high, while in the case II it is low. The case III represent a plasma which has a large three-body recombination rate.

Numerical results obtained from (1), (2) and (3) are given as a function of time. The quasi-steady state assumption is made for all levels $i > i^*$. The level i^* is determined so as to satisfy the following two conditions: (a) $i^* \geqq 5$, and (b) the relaxation time for n_i with $i \geqq i^* + 1$ is less than one hundredth of an apparent relaxation time for the electron energy estimated from (3), that is,

$$1.5\, n_e T_e/(-R_e - Q_e + 1.5\, T_e\, \mathrm{d}n_e/\mathrm{d}t)\,.$$

Table 1. Initial conditions.

	T_{e0}	T_{i0}	n_{e0}	T_{a0}	n_{10}
I	10 eV	0.1 eV	10^{13} cm^{-3}	0.1 eV	10^{17} cm^{-3}
II	10	0.1	10^{13}	0.1	0.9×10^{14}
III	10	0.1	10^{14}	0.1	10^{17}

Integration of the equations was performed by using the Runge-Kutta-Gill method. The time step Δt was set to be one tenth of the relaxation time for the population density of the level i^*. To see the effect of Δt on the numerical results, we also made the calculation in the case II by using Δt equal to one hundredth of the relaxation time for the level i^*, and found that the two results agree, reasonably well.

3. Numerical Results and Discussion

We describe population inversion between the levels with principal quantum number 3 and 4 as a representative case.

Figure 1 shows T_e, T_i and T_a as functions of time t, respectively, in the plasma which is interacting with the neutral gas. The electron temperature in the cases I and III rapidly decreases down to about 0.2 eV in 10^{-7} s (Figure 1a). All the temperatures are relaxed to 0.10 eV in the case I and 0.11 eV in the case III. We will call these temperatures the "relaxed temperatures". Since n_e is higher by one order of magnitude in the case III than in the case I, the relaxed temperature becomes slightly higher. On the other hand, T_e is decreased more slowly in the case II (Fig. 1b), and the relaxed temperature is 0.40 eV. This is because n_{10} is significantly lower by two orders of magnitude in the case II than in the cases I and III. Detailed description of the elastic and inelastic collisional effects on the variation of T_e is given in Appendix B.

Figure 2 shows n_i/ω_i ($i = 1, 2, 3$ and 4) and n_e versus t where ω_i is the statistical weight of level i. In the case I (Fig. 2a) n_e changes only slightly till $t \approx 10^{-5}$ s, then decreases by more than one order of magnitude in about 1 ms. The population densities of the levels 3 and 4 make rapid increases and falls till $t \approx 2 \times 10^{-7}$ s, and, after then, again increase slightly till $t \approx 10^{-5}$ s. Finally, the population inversion between the two levels appear after $t \approx 2 \times 10^{-5}$ s. In the case III (Fig. 2a), similar behaviours are obtained. The corresponding plots for the case II are shwon in Fig. 2b. In order to show the evolution of the population inversion clearly, we plot the overpopulation density, $\Delta n_{43} = n_4/\omega_4 - n_3/\omega_3$, for times $t > t_Q$ in Fig. 2c.

Figure 3 shows $\dot{n}_i \equiv \mathrm{d}n_i/\mathrm{d}t$ ($i = 1, 2, 3$ and 4) and $\dot{n}_e \equiv \mathrm{d}n_e/\mathrm{d}t$ versus t. The solid curves represent the positive values of $\dot{n}_i$ and $\dot{n}_e$, while the dotted curves

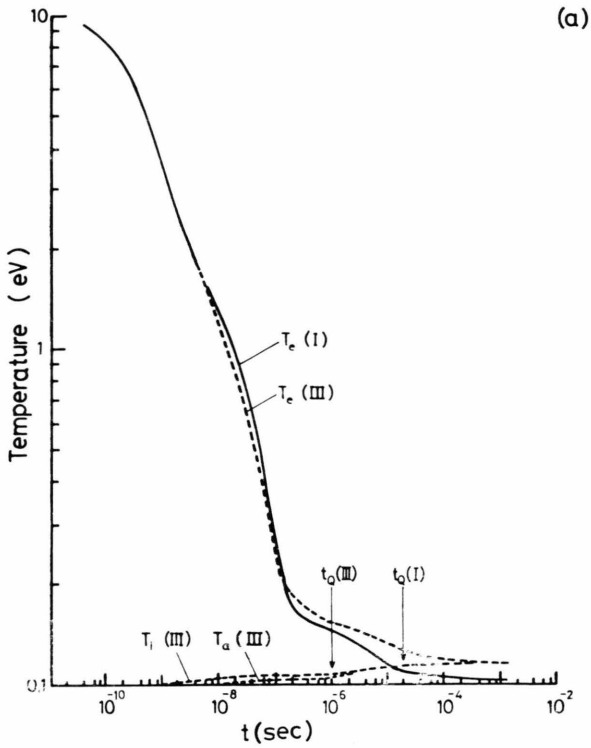

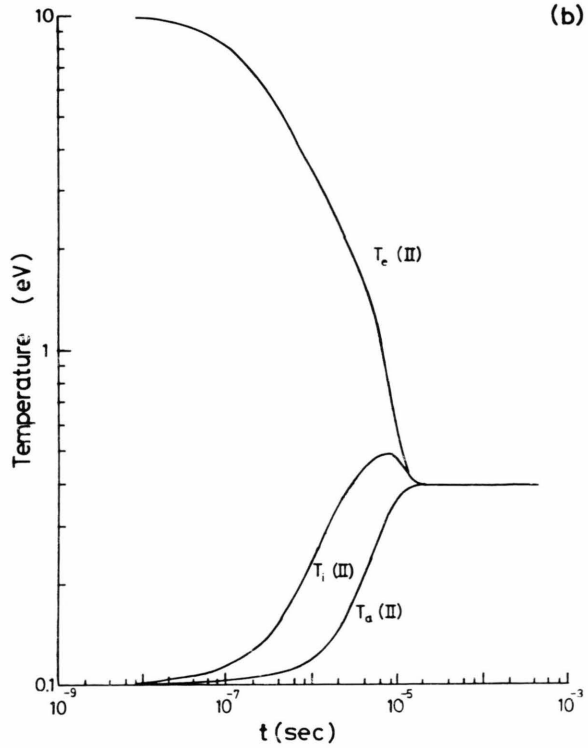

Fig. 1. Electron, ion and atom temperature *vs.* time. (a): the cases I and III. (b): The case II. "T (I)" means temperature in the case I, etc. The arrows labeled t_Q (I) and t_Q (III) show times of establishment of QSS in the cases I and III, respectively. The corresponding time for the case II is shown by the arrow marked t_Q (II) (see Figs. 2 and 3).

represent the negative values of $\dot{n}_i$ and $\dot{n}_e$. The times during which $\dot{n}_e > 0$ and $\dot{n}_e < 0$ correspond to the ionizing phase and the recombining phase of the plasma, respectively. It is seen from Fig. 3 that QSS, i.e., $\dot{n}_i \approx -\dot{n}_e$, is finally established after 2.0×10^{-5} s in the case I (Fig. 3a) and after 1.5×10^{-5} s in the case II (Fig. 3b), while in the case III, QSS is realized most quickly at 1.0×10^{-6} s.

Cacciatore, Capitelli and Drawin [17] estimated the time t_Q required for QSS to be established under constant temperature conditions in a hydrogen plasma, with the initial population densities in Saha equilibrium. For example, $t_Q = 2 \times 10^{-7}$ s at $T_e = 1.4$ eV and $n_e = 10^{12}$ cm^{-3}. Our calculated t_Q under temporal variation of the temperature is significantly longer than that by Cacciator, Capitelli and Drawin. The temporal variation of the temperature becomes sufficiently small when QSS is established, as shown in Figs. 1 and 3. In other words, the high-temperature hydrogen plasma which is interacting with the low-temperature, high-density hydrogen gas becomes QSS when the temperatures reach an equilibrium level. This means that the QSS approximation is not valid when the temporal variation of the temperature is large.

As shown in Fig. 2, population inversion takes place after QSS is established. The population inversion is not produced in the transient recombining phase. This is explained as follows: The electrons in the plasma which is interacting with the cold and dense neutral hydrogen gas are rapidly cooled to nearly the equilibrium temperature. In the early period ($t \lesssim 10^{-7}$ s) of the case I as example, however, the plasma is in a transient ionizing phase, since the population density of the ground state of the hydrogen atom is large and the excitation and ionization are induced by the electron impact (see Figs. 1a ~ 3a). In this situation the population inversion cannot be produced. The transient recombining phase follows the ionizing phase (see Figure 3a). The ion density n^+, which is equal to n_e, is only slightly increased from the initial value, and

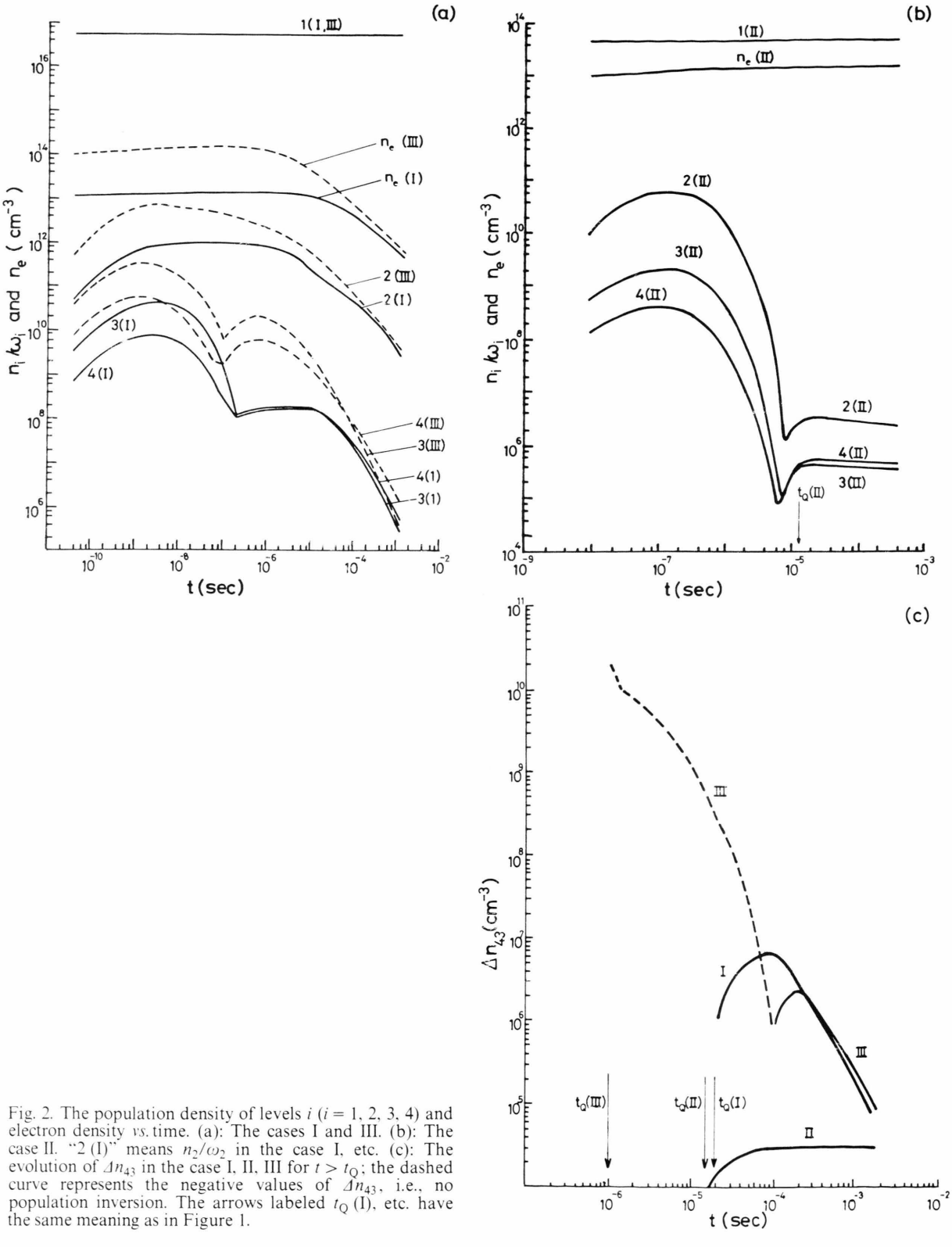

Fig. 2. The population density of levels i ($i = 1, 2, 3, 4$) and electron density *vs.* time. (a): The cases I and III. (b): The case II. "2 (I)" means n_2/ω_2 in the case I, etc. (c): The evolution of Δn_{43} in the case I, II, III for $t > t_Q$; the dashed curve represents the negative values of Δn_{43}, i.e., no population inversion. The arrows labeled t_Q (I), etc. have the same meaning as in Figure 1.

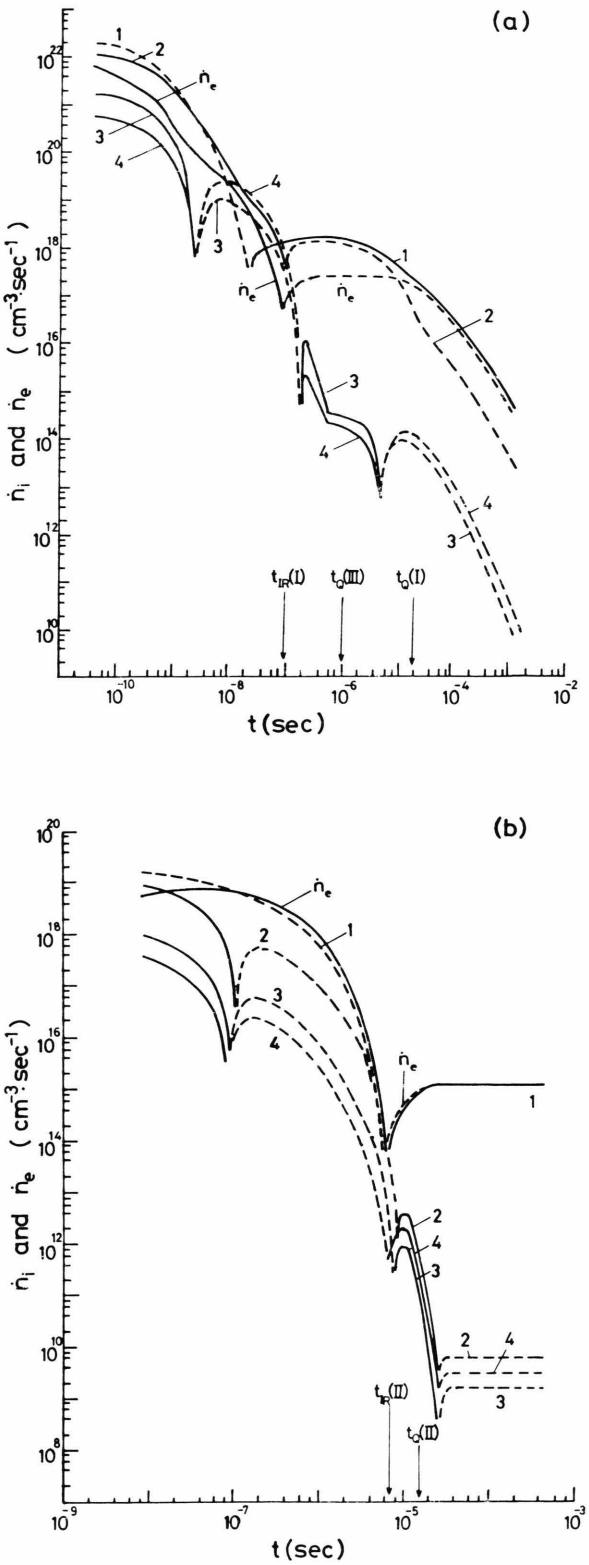

Fig. 3. The rate of increase in the population density of levels i ($i = 1, 2, 3, 4$) and electron density. The solid and dashed lines denote growing and decreasing rates, respectively. (a): The case I. (b): The case II. "i" means dn_i/dt. The arrows labeled t_{IR} denote a time when the ionizing phase in the earlier time changes to the recombining one. The other arrows labeled t_Q (I), etc. have the same meaning as in Figs. 1 and 2.

T_e is decreased only by about 0.1 eV in this phase (see Figs. 1 a ~ 3 a). This means that the three-body recombination is hardly increased in the transient recombining phase. Population inversion is not expected, since the populating rate for the level 4 from the upper levels is not much increased.

If the high-temperature hydrogen plasma is brought into contact with an other neutral gas instead of hydrogen gas, population inversion is expected even in the transient recombining phase because the population density of the ground state of the hydrogen atoms is not increased at all in this case.

At $n_{e0} = 10^{13}\,\mathrm{cm}^{-3}$ (case I and II), population inversion between levels 3 and 4 is produced immediately after quasi-steady state is realized. At $n_{e0} = 10^{14}\,\mathrm{cm}^{-3}$ (case III), however, the population inversion is not produced till $t = 10^{-4}$ s in the quasi-steady state. These facts indicate that the electron temperature and density of the plasma must be in the region for the inversion shown in [7–9] (for example, see Fig. 1 in [8]).

In the case I and III, the overpopulation density $\Delta n_{43} \equiv (n_4/\omega_4 - n_3/\omega_3)$ is rather high while the electron density is high, because the three-body recombination rate is enlarged at the low relaxed-temperature. But large decrease in n_e against time significantly reduces Δn_{43} itself. In the case II, Δn_{43} keeps almost constant in quasi-steady state, but small in magnitude, because the high relaxed-temperature keeps $|\dot{n}_e|$ relatively small. For small n_1 accompanying the high relaxed-temperature as in the case II, the population inversion can be easily produced because of the small self-absorption of the Lyman series. But the overpopulation density is small in magnitude (see Fig. 2), since the high relaxed-temperature keeps $|\dot{n}_e|$ relatively small.

When the initial temperature of the plasma is high, the relaxed temperature, after the neutral gas is introduced, is also high. In the present case, the population inversion takes place in the QSS. Since the three-body recombination process plays a dominant role for the population inversion in the

high density QSS plasma, the overpopulation density becomes low when the relaxed temperature is high. The detailed discussion has been already given in [11]. When the initial electron density of the plasm is high and the population inversion is not immediately realized in QSS, the relaxed temperature is higher than the case produced immediately in QSS: the relaxed temperature in the case III is higher (0.11 eV) than in the case I (0.1 eV). Therefore, in this case the maximum value of overpopulation density becomes low.

4. Conclusion

For the recombining hydrogen plasma which is interacting with cool and dense neutral hydrogen gas, we have obtained the following results:

1. Under our initial conditions, it takes a rather long time for QSS to be established. In other words, the population densities change rapidly in time during the transient recombining phase. A QSS approximation would yield large errors in the population densities when applied to these initial conditions.

2. The population inversion cannot be expected in the transient recombining phase, but is realized only in QSS and in the region for the electron density and temperature shown in [7–9].

3. When the initial electron temperature of the plasma is high, the overpopulation density becomes low, since the relaxed temperature is rather high. When the initial electron density is high and the population inversion is not immediately produced even in QSS, the maximum value of overpopulation density cannot be high, since the relaxed temperature is also high in this case.

4. QSS cannot be realized while intense energy-flows due to the collisional processes exist between different kinds of the particles in the plasma.

Acknowledgements

This study was carried out as a part of collaborating research at the Institute of Plasma Physics, Nagoya University. The numerical calculations have been made at the Computer Center of the Institute of Plasma Physics, Nagoya University and at the Computer Center in Kyushu University and at the Computer Center in Ehime University.

Appendix A

Besides the elastic collisional processes, elementary reaction processes considered in the energy equation are given in Eqs. (a) ~ (e) in § 2.

We make the following assumptions for the transfer of energy between the various particles due to the collisional and radiative processes:

1. In the excitation processes (a_1) and (d_1), the kinetic energy of the excited atom does not change before and after the reaction. The excitation energy

Table 2. Rate of increase of thermal energy for each elementary reaction process.

	Reaction process	Q_e	Q_i	Q_a
(a_1)	$H_j + e \rightarrow H_k + e \ (k > j)$	$-n_e \sum_{j<k} \sum (E_j - E_k) C_{jk} n_j$		
(a_2)	$\leftarrow$	$n_e \sum_{j<k} \sum (E_j - E_k) F_{kj} n_k$		
(b_1)	$H_j + e \rightarrow H_+ + e + e$	$-n_e \sum_j E_j K_{jc} n_j$	$\frac{3}{2} T_a n_e \sum_j K_{jc} n_j$	$-\frac{3}{2} T_a n_e \sum_j K_{jc} n_j$
(b_2)	$\leftarrow$	$n_e^3 \sum_j E_j K_{cj}$	$-\frac{3}{2} T_i n_e^3 \sum_j K_{cj}$	$\frac{3}{2} T_i n_e^3 \sum_j K_{cj}$
(c)	$H_+ + e \rightarrow H_j + h\nu$	$-\frac{3}{2} T_e n_e^2 \sum_j \Lambda_j \beta_j$	$-\frac{3}{2} T_i n_e^2 \sum_j \Lambda_j \beta_j$	$\frac{3}{2} T_i n_e^2 \sum_j \Lambda_j \beta_j$
(d_1)	$H_j + N \rightarrow H_k + N \ (k > j)$			$-n_1 \sum_{j<k} \sum (E_j - E_k) C^0_{jk} n_j$
(d_2)	$\leftarrow$			$n_1 \sum_{j<k} \sum (E_j - E_k) F^0_{kj} n_j$
(e_1)	$H_j + N \rightarrow H_+ + e + N$	0	$\frac{3}{2} n_1 T_a \sum_j K^0_{jc} n_j$	$-n_1 \sum_j (\frac{3}{2} T_a + E_j) K^0_{jc} n_j$
(e_2)	$\leftarrow$	0	$-\frac{3}{2} n_1 n_e^2 T_i \sum_j K^0_{cj}$	$n_1 n_e^2 \sum_j (\frac{3}{2} T_i + E_j) K^0_{cj}$

is supplied by the electron in the process (a_1), and by the ground-state atom in the process (d_1).

2. In the ionization processes (b_1) and (e_1), the kinetic energy of the excited atom is transferred to that of the ion without any loss. The ionization energy is supplied by the electron in the process (b_1), and by the ground state atom in the process (e_1). We neglect the kinetic energy of the released electrons in both processes (b_1) and (e_1).

3. In the deexcitation processes (a_2) and (d_2) and the recombination processes (b_2) and (e_2), all the corresponding energy reactions are regarded as the inverse reactions in the processes (a_1), (d_1), (b_1) and (e_1), respectively.

4. The excess energy released in the inelastic radiative recombination process (c) is carried off by the photon.

Table 2 shows the increase rates of the thermal energy Q of the electrons, the ions and the atoms, which are expressed by using the ionization energy E_j from the level j, the population density n_j and the rate coefficient of each process.

By using the relation

$$\frac{dn_e}{dt} = \frac{dn^+}{dt} = -\sum_j \frac{dn_j}{dt} = \sum_j (n_e K_{jc} + n_1 K_{jc}^0) n_j - n_e^2 \sum_j (n_e K_{cj} + \Lambda_j \beta_j + n_1 K_{cj}^0),$$

we obtain the following energy equations:

- for electrons,

$$\frac{dT_e}{dt} = \frac{1}{\tau_{ea}}(T_a - T_e) + \frac{1}{\tau_{ei}}(T_i - T_e) + \frac{2}{3}\left[-\sum_{k=2}^{20}\sum_{j=1}^{k-1}(E_j - E_k)(C_{jk} n_j - F_{kj} n_k) - \sum_{j=1}^{20}(E_j + \tfrac{3}{2} T_e) K_{jc} n_j + n_e^2 \sum_{j=1}^{20}(E_j + \tfrac{3}{2} T_e) K_{cj} - \tfrac{3}{2} T_e \frac{n_1}{n_e} \sum_{j=1}^{20}(K_{jc}^0 n_j + n_e^2 K_{cj}^0)\right], \quad \text{(A.1)}$$

- for ions

$$\frac{dT_i}{dt} = \frac{1}{\tau_{ia}}(T_e - T_i) + \frac{1}{\tau_{ie}}(T_e - T_i) + (T_a - T_i)\sum_{j=1}^{20}\left(K_{jc} + K_{jc}^0 \frac{n_1}{n_e}\right) n_j, \quad \text{(A.2)}$$

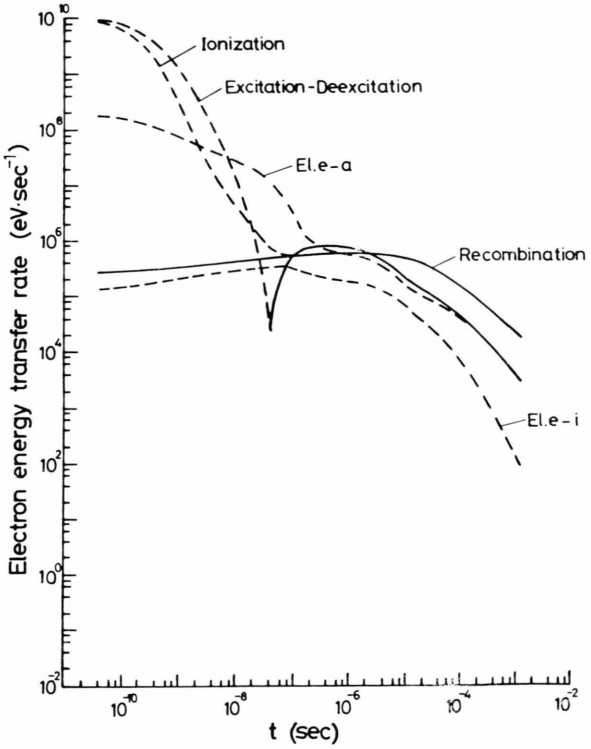

Fig. 4. Electron energy transfer rate due to elastic and inelastic collisions for the case I. The solid and dashed lines denote the incoming and the outgoing energy fluxes respectively. "El. e−a" means the transfer rate by electron-atom elastic collisions.

- and for atoms

$$\frac{dT_a}{dt} = \frac{1}{\tau_{ia}}(T_i - T_a) + \frac{1}{\tau_{ea}}(T_e - T_a) + \frac{2}{3}\frac{n_1}{n_a}\left[-\sum_{k=2}^{20}\sum_{j=1}^{k-1}(E_j - E_k)(C_{jk}^0 n_j - F_{kj}^0 n_k) - \sum_{j=1}^{20} E_j (K_{jc}^0 n_j - K_{cj}^0 n_e^2) + \tfrac{3}{2}(T_i - T_a)\frac{n_e^2}{n_1} \cdot \sum_{j=1}^{20}(n_e K_{cj} + \Lambda_j \beta_j + n_1 K_{cj}^0)\right]. \quad \text{(A.3)}$$

Fig. 5. Electron energy transfer rate due to inelastic collisions for the case I. The solid and dashed lines denote the incoming and outgoing energy fluxes, respectively. "$j \to k$" denotes the transition from jth level to the kth level, and "C" denotes continuum state. (a) the electron energy loss rate for the excitation processes. (b) the electron energy loss rate for the ionization processes. (c) the electron energy gain rate for the deexcitation processes. (d) the electron energy gain rate for the three-body recombination processes.

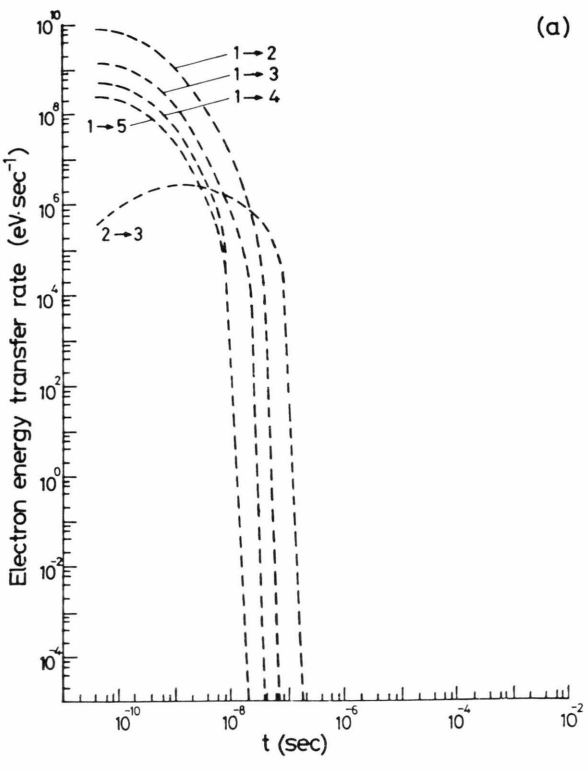
(a)
Electron energy transfer rate (eV·sec⁻¹)
t (sec)
1→2
1→3
1→4
1→5
2→3

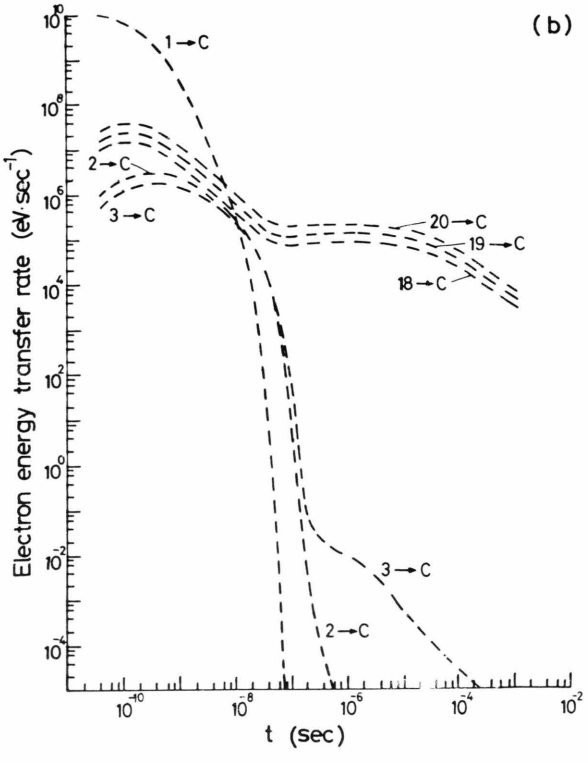
(b)
Electron energy transfer rate (eV·sec⁻¹)
t (sec)
1→C
2→C
3→C
20→C
19→C
18→C

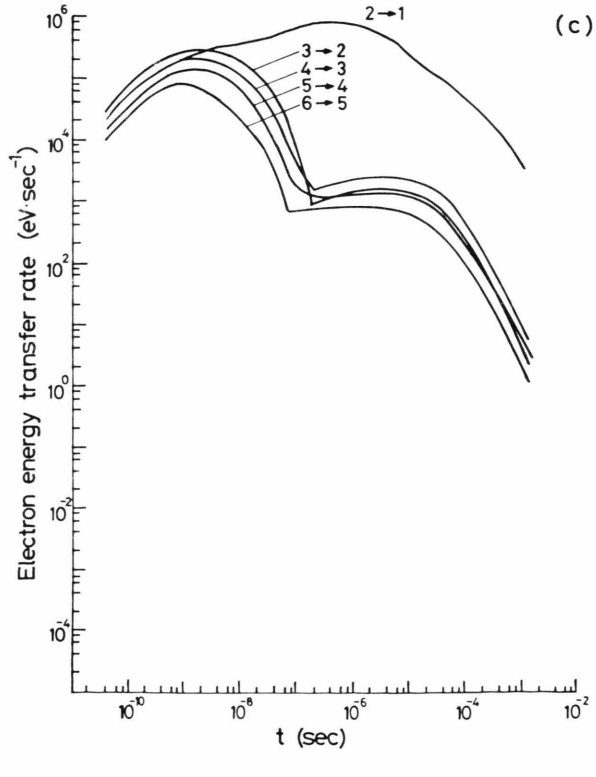
(c)
Electron energy transfer rate (eV·sec⁻¹)
t (sec)
2→1
3→2
4→3
5→4
6→5

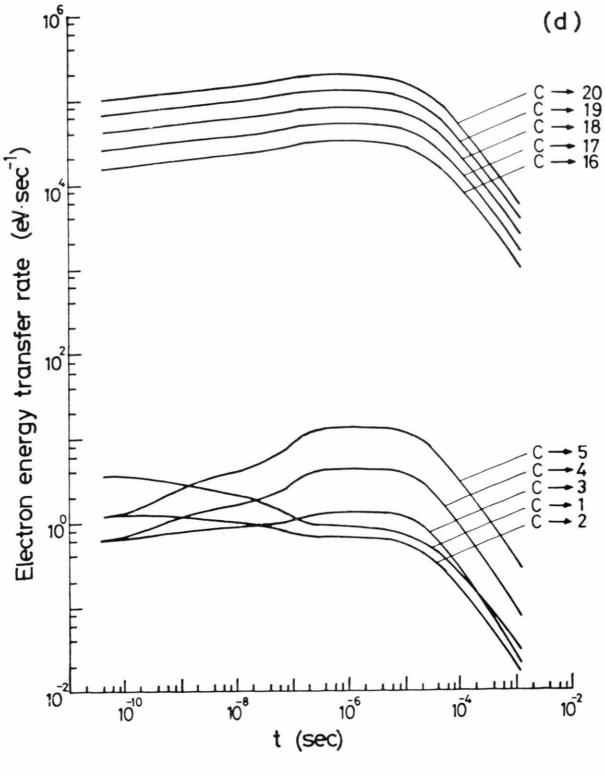
(d)
Electron energy transfer rate (eV·sec⁻¹)
t (sec)
C→20
C→19
C→18
C→17
C→16
C→5
C→4
C→3
C→1
C→2

The first and second terms on the R.H.S. of the above energy equations are the transfer rates of the energy due to elastic collisions, the electron-ion collision time (τ_{ei}) is given in (5−21) of [18], the electron-atom and ion-atom collision times (τ_{ea} and τ_{ia}) are calculated, respectively, by using the result of [19].

Appendix B

Figure 4 shows the electron energy transfer rates due to elastic and inelastic collisions for the case I as a typical case. In very early times ($t < 10^{-9}$ s), the energy loss is mainly due to the ionization and the excitation processes. After then, the elastic collision process between the electrons and the atoms becomes dominant. When the ionizing phase changes to the recombining one (see Fig. 3), the energy gain due to the three-body recombination process becomes comparable to the energy loss by the ionization process.

Transfer rates for energy loss and gain between various levels including the continuum levels are shown in Figure 5. In the higher electron temperature range, the energy loss by electronic excitation collisions from the ground state to level 2 (see Fig. 5a) and electron ionization collisions from the ground state (see Fig. 5b) are dominant. In the nearly relaxed low electron temperature range, the energy is mainly lost by electron-impact ionization collisions from the higher levels (see Figure 5b). The energy transfer rates due to elastic collisions and other electron inelastic collisions are not negligible in the electron energy rate. Particularly, in the low electron temperature range the energy gain due to electron deexcitation from level 2 to the ground state is the greatest in comparison with that between the other energy levels (see Figure 5c). In the whole electron temperature range, the electron energy gain due to three-body recombination into the upper levels is dominant compared with the one into the lower lying levels (see Figure 5d).

[1] L. T. Gudzenko and L. A. Shelepin, Sov. Phys. JETP **18,** 998 (1964).
[2] E. M. Campbell, R. G. Jahn, W. F. von Jaskowsky, and K. E. Clark, Appl. Phys. Lett. **30,** 575 (1977).
[3] T. Hara, K. Kodera, M. Hamagaki, K. Matsunaga, M. Inutake, and T. Dote, Japan J. Appl. Phys. **19,** L606 (1980).
[4] S. Suckewer, R. J. Hawryluk, M. Okabayashi, and J. A. Schmidt, Appl. Phys. Lett. **29,** 537 (1976).
[5] K. Sato, M. Shibo, M. Hosokawa, H. Sugawara, T. Oda, and T. Sasaki, Phys. Rev. Lett. **39,** 1074 (1977).
[6] A. A. Skorupski and S. Sukewer, Phys. Lett. **A 46,** 473 (1974).
[7] W. L. Bohn, Appl. Phys. Lett. **24,** 15 (1974).
[8] U. Furukane, T. Yokota, and T. Oda, J. Quant. Spectr. Radiat. Transfer, **22,** 239 (1979).
[9] U. Furukane and T. Yamamoto, Japan J. Appl. Phys. **19,** L285 (1980).
[10] U. Furukane, T. Yokota, K. Kawasaki, and T. Oda, J. Quant. Spectr. Radiat. Transfer **29,** 75 (1983).
[11] T. Oda and U. Furukane, J. Quant. Spectr. Radiat. Transfer **29,** 553 (1983).
[12] P. Hoffman and W. L. Bohn, Z. Naturforsch. **22a,** 1953 (1967).
[13] M. Otsuka, R. Ikee, and K. Ishii, J. Quant. Spectr. Radiat. Transfer, **15,** 995 (1975).
[14] M. Otsuka, R. Ikee, and K. Ishii, J. Quant. Spectr. Radiat. Transfer **21,** 41 (1979).
[15] M. Cacciatore and M. Capitelli, Z. Naturforsch. **29a,** 1507 (1974).
[16] H. W. Drawin, F. Emard, and K. Katsonis, Z. Naturforsch. **28a,** 1422 (1973).
[17] M. Cacciatore, M. Capitelli, and H. W. Drawin, Physica **84c,** 267 (1976).
[18] L. Spitzer, Jr., Physics of Fully Ionized Gases, 2nd Ed. p. 135. Wiley Intersci., New York 1961.
[19] D. Düchs and H. R. Girem, Phys. Fluids **9,** 1099 (1966).